

Nonequilibrium transport through the Hubbard dimer

Yaroslav Pavlyukh¹ and Riku Tuovinen²

¹Institute of Theoretical Physics, Faculty of Fundamental Problems of Technology, Wrocław University of Science and Technology, Wrocław, 50-370, Poland.

²Department of Physics, Nanoscience Center, University of Jyväskylä, P.O. Box 35, 40014, Finland.

Contributing authors: yaroslav.pavlyukh@pwr.edu.pl;
riku.m.s.tuovinen@jyu.fi;

Abstract

We apply a computationally efficient approach to study the time- and energy-resolved spectral properties of a two-site Hubbard model using the nonequilibrium Green's function formalism. By employing the iterative generalized Kadanoff-Baym ansatz (iGKBA) within a time-linear framework, we avoid the computational cost of solving the full two-time Kadanoff-Baym equations. Spectral information is extracted by coupling the system to multiple narrow-band leads, establishing a direct analogy to photoemission experiments. Our results reveal correlation-induced shifts and broadenings of spectral features, along with a suppression of transient current oscillations. This approach provides a promising avenue for analyzing correlated electron dynamics in open quantum systems.

Keywords: quantum transport, ultrafast phenomena, correlated systems, nonequilibrium Green's function theory, generalized Kadanoff-Baym Ansatz

1 Introduction

Hubbard model [1] is one of the most studied models of strongly correlated systems. It is traditionally used as a testbed of new approximations and numerical methods. As an open quantum system it was used in demonstrating heat transfer mechanisms [2, 3] and

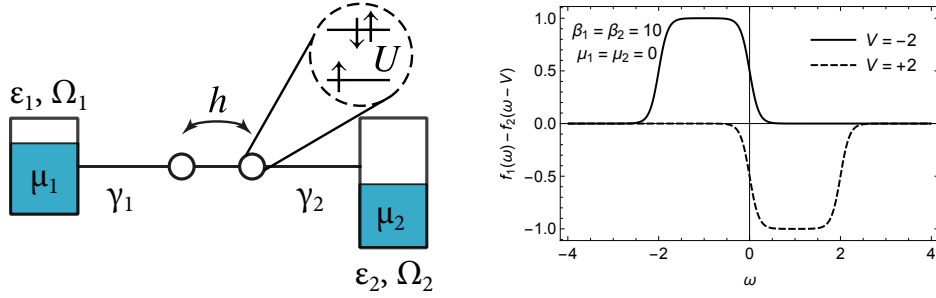


Fig. 1 Left: system setup consisting of a Hubbard dimer connected to two leads with different chemical potentials μ_α , energy centroids ϵ_α and bandwidths Ω_α , right: difference of the distribution functions in a biased system — ingredient of the Landauer-Büttiker formula (Eq. 19) for steady-state currents.

in studies of thermoelectricity [4, 5]. The focus of this work is the so-called Hubbard dimer, i.e., a model with two sites in contact with electronic reservoirs (Fig. 1, left).

In our previous work [6], based on the nonequilibrium Green’s function (NEGF) approach, we demonstrated that coherent electron dynamics of the isolated Hubbard dimer can be studied analytically in four important approximations: second Born, GW , and two flavors of T -matrix approximation. It was shown that the off-diagonal elements of the density matrix satisfy oscillator-like equations of motion. This enabled us to derive analytical expansions for the system’s equilibrium properties, as reached through an adiabatic switching protocol starting from a non-interacting initial state. This approach serves as an alternative to equilibrium many-body perturbation theory (MBPT) [7–9].

A crucial ingredient of these derivations is the generalized Kadanoff–Baym ansatz (GKBA) [10] which reduces the complex integro-differential Kadanoff–Baym equations (KBE) to a set of coupled ordinary differential equations (ODE) [11–13]. The strength of the GKBA+ODE formulation lies in its linear scaling with physical propagation time. This significantly pushes the limits of NEGF approach as compared to solving integro-differential KB equations, which scale cubically with physical time. However, GKBA represents the lesser/greater Green’s functions (GFs) in a simplified form,

$$G^{\lessgtr}(t, t') = -G^R(t, t')\rho^{\lessgtr}(t') + \rho^{\lessgtr}(t)G^A(t, t'), \quad (1)$$

typically using a mean-field retarded propagator (specified below):

$$G^R(t, t') = -i\theta(t - t')T \left\{ e^{-i \int_{t'}^t d\tau h_{\text{HF}}(\tau)} \right\}. \quad (2)$$

This makes it impossible to retrieve the spectral information contained in the full two-times GFs, $G^{\lessgtr}(t, t')$. The limitation is significant because many experimental techniques rely on spectral information to probe electronic properties.

Multidimensional coherent spectroscopies [14–16] provide a direct way to access two-time correlation functions by measuring system responses to sequences of ultrafast optical pulses. These techniques are particularly useful for studying coherent electronic

dynamics but require sophisticated setups capable of resolving temporal correlations explicitly.

In contrast, photoemission spectroscopies [17, 18] do not measure two-time correlation functions directly. Instead, they provide access to electronic spectral properties by detecting emitted electrons and recording their energies. The measured signal reflects the density of states, integrated over the measurement time window, rather than explicit time-dependent correlations. Since theories based on single-time correlators cannot naturally recover two-time spectral information, modeling photoemission within such frameworks requires an alternative approach — namely, the introduction of an energy-selective detection mechanism.

To achieve this, we model detectors as an *embedding* characterized by the tunneling matrix elements $T_{ik\alpha}$ between the system state i and an environmental state k in electronic lead α with energy $E_{k\alpha}$. Since perfectly energy-selective detectors are unphysical, we describe the associated tunneling rate using a peaked function (Lorentzian distribution):

$$\Gamma_{\alpha,ij}(\omega) = \sum_k T_{ik\alpha} T_{k\alpha j} \delta(E_{k\alpha} - \omega) = \frac{\gamma_{\alpha,ij} \Omega_\alpha^2}{(\omega - \epsilon_\alpha)^2 + \Omega_\alpha^2}, \quad (3)$$

which is centered at ϵ_α with width Ω_α . Similar concepts have been employed previously, for example, in Ref. [19], where a continuum embedding was used to describe photoemission from a quasiparticle peak and its plasmon satellite. However, extending this approach to capture transient dynamics across a broad energy range requires an efficient method for propagating the system's state in time. With the advent of time-linear GKBA-based methods, such modeling becomes computationally feasible. To illustrate the potential of this approach, we apply it to study bias-driven transient dynamics in a Hubbard dimer.

The outline of this work is as follows: In Sec. 2, we introduce the GKBA+ODE approach. We begin with a description of correlated electron dynamics in closed systems and then generalize it to open systems in contact with a structured environment. Next, we review the electronic properties of the two-site Hubbard model. In Sec. 3, we present our results, focusing on time- and energy-resolved currents. Finally, in Sec. 4, we summarize our findings.

2 Theory

2.1 Time-linear nonequilibrium Green's function formalism

In the NEGF formalism, the electronic lesser/ greater single-particle Green's functions

$$G_{ij}^<(t, t') = i \langle \hat{d}_j^\dagger(t') \hat{d}_i(t) \rangle, \quad G_{ij}^>(t, t') = -i \langle \hat{d}_i(t) \hat{d}_j^\dagger(t') \rangle, \quad (4)$$

are the fundamental correlators giving rise to various physical observables. The annihilation and creation operators $\hat{d}^{(\dagger)}$ will be specified later with the model description. In time-linear ODE formulations, instead of solving the full two-times Kadanoff-Baym

equations:

$$[i\partial_t - h(t)] G^{\lessgtr}(t, t') = \left[\Sigma^{\lessgtr} \cdot G^A + \Sigma^R \cdot G^{\lessgtr} \right](t, t'), \quad (5)$$

where $[A \cdot B](t, t') \equiv \int d\bar{t} A(t, \bar{t}) B(\bar{t}, t')$, is a real-time convolution, $X^{R/A}(t, t')$ are the retarded/advanced functions, and Σ is the correlation part of the self-energy, one aims to find a system of equations for the time-diagonal of GFs, which are the densities:

$$\rho_{ij}^{\lessgtr}(t) = -iG_{ij}^{\lessgtr}(t, t). \quad (6)$$

Combining Eq. (5) with its adjoint and going to the equal times limit one obtains:

$$\frac{d}{dt} \rho^<(t) = -i[h_{\text{HF}}(t), \rho^<(t)] - (I(t) + I^\dagger(t)), \quad (7)$$

where $h_{\text{HF}}(t) = h(t) + V_{\text{HF}}(t)$ is the Hartree-Fock Hamiltonian. The mean-field potential is given by

$$V_{\text{HF},ij}(t) = \sum_{mn} w_{imnj} \rho_{nm}^<(t), \quad (8)$$

with $w_{imnj} = v_{imnj} - v_{imjn}$, and v_{imnj} being the Coulomb matrix elements. The collision term is expressed in terms of the two-particle Green's function (2-GF)

$$I_{lj}(t) = I_{lj}^c(t) = -i \sum_{imn} v_{lnmi}(t) \mathcal{G}_{imjn}(t), \quad (9)$$

which is a functional of the two-times $G^{\lessgtr}(t, t')$ and which can be expressed in terms of $\rho_{ij}^{\lessgtr}(t)$ with the help of GKBA using an appropriate approximation for the correlated self-energy. The procedure is described in detail in Ref. [20], and its application to the Hubbard dimer is given in Ref. [6]. In the present work we focus on the so-called second Born approximation for the electron self-energy. This approximation works very well for the dimer at half-filling as demonstrated for spectral properties [21] and densities [6]. Extensive comparison of the self-energy approximations out of equilibrium was performed by Schlünzen *et al.* [22, 23].

Besides electronic correlations, the GKBA+ODE approach can also incorporate other physical processes, such as interaction with bosonic particles [24] and environment [25]. In this case, the integral $I(t)$ becomes a sum of different collision mechanisms. It was shown that interaction with cavity photons gives rise to the Autler-Townes spectral features [26] and is manifested in the high harmonics spectrum excited in a transport setup [27]. In this work, we focus on the interplay of electronic correlations and transport, therefore the collision integral consists of the correlation (c) and embedding (em) terms

$$I(t) = I^c(t) + I^{\text{em}}(t). \quad (10)$$

For wide-band leads, i.e., $\Omega_\alpha \rightarrow \infty$, the embedding self-energy takes a simple form [28]

$$\Sigma_\alpha^R(t, t') = -\frac{i}{2} s_\alpha^2(t) \delta(t, t') \gamma_\alpha, \quad (11a)$$

$$\Sigma_\alpha^<(t, t') = i s_\alpha(t) s_\alpha(t') e^{-i\phi_\alpha(t, t')} \int \frac{d\omega}{2\pi} f_\alpha(\omega) e^{-i\omega(t-t')} \gamma_\alpha, \quad (11b)$$

where $s_\alpha(t)$ is the switch-on function for the contact between the system and electrode α , $\phi_\alpha(t, t') \equiv \int_{t'}^t d\bar{t} V_\alpha(\bar{t})$ is the accumulated phase due to the time-dependent voltage V_α , and $f_\alpha(\omega) = 1/(e^{\beta_\alpha(\omega - \mu_\alpha)} + 1)$ is the Fermi function at inverse temperature β_α and chemical potential μ_α . Expanding into the partial fractions [29]

$$f_\alpha(\omega) = \frac{1}{2} - \sum_{\ell \geq 1} \eta_\ell \left[\frac{1}{\beta_\alpha(\omega - \mu_\alpha) + i\zeta_\ell} + \frac{1}{\beta_\alpha(\omega - \mu_\alpha) - i\zeta_\ell} \right], \quad \text{with } \text{Re } \zeta_\ell > 0, \quad (12)$$

allows to express $I^{\text{em}}(t)$ in terms of an embedding correlator $\mathcal{G}^{\text{em}}(t)$ [25]

$$I^{\text{em}}(t) = -\frac{1}{4} \Gamma(t) - \sum_{\ell \alpha} s_\alpha(t) \frac{\eta_\ell}{\beta_\alpha} \Gamma_\alpha \mathcal{G}_{\ell \alpha}^{\text{em}}(t) \quad (13)$$

that fulfills the equation of motion:

$$i \frac{d}{dt} \mathcal{G}_{\ell \alpha}^{\text{em}}(t) = -s_\alpha(t) - \mathcal{G}_{\ell \alpha}^{\text{em}}(t) \left(h_{\text{eff}}^\dagger(t) - V_\alpha(t) - \mu_\alpha + i \frac{\zeta_\ell}{\beta_\alpha} \right). \quad (14)$$

Here, $h_{\text{eff}}(t) \equiv h_{\text{HF}}(t) - i\Gamma(t)/2$ is the effective mean-field Hamiltonian and $\Gamma(t) = \sum_\alpha s_\alpha^2(t) \gamma_\alpha$. This approach was recently generalized [30] towards finite widths spectral densities (Eq. 3) incorporating reconstructions [31–34] of $G^{\leq}(t, t')$ on the level beyond GKBA (Eq. 1). The generalization, referred to as the *iterated generalized Kadanoff-Baym ansatz* (*iGKBA*), follows the same basic principles, albeit at the cost of introducing additional correlators. These correlators must be co-propagated alongside the equation of motion for the density (7), contributing to the electron dynamics and enabling the determination of the time-resolved electronic currents through a generalization of the Meir, Wingreen and Jauho [35, 36] formula.

The computational complexity of propagating $\mathcal{G}_{imjn}(t)$ and computing the electronic collision integral $I^c(t)$ is $\mathcal{O}(N_{\text{e-basis}}^5 N_t)$, where N_t is the number of time-steps. The computational complexity of the embedding collision integral $I^{\text{em}}(t)$ at the *iGKBA* level is $\mathcal{O}(N_{\text{e-basis}}^3 N_{\text{leads}}^2 (2N_{\text{leads}} + 4N_p) N_t)$, where N_p is the number of poles in the expansion (12) of the Fermi-Dirac distribution function. This is comparable with the cost of solving the Dyson equation for the equilibrium Green's function. This approach typically consists of evaluating the second Born self-energy and solving the Dyson equation until self-consistency is achieved. The self-energy is typically evaluated in the imaginary time-domain on a grid of N_τ points with $\mathcal{O}(N_{\text{e-basis}}^5 N_\tau)$ complexity [37]. The scaling of solving the Dyson equation strongly depends on the domain

and representation, as reviewed in Ref. [38]. The analytic continuation of the Green's function from imaginary to real frequency, which is an important ingredient of such an approach, is a separate and intensely investigated issue [39].

2.2 System

Before applying the *i*GKBA method to the Hubbard dimer, let us recall its relevant electronic properties. Its Hamiltonian in the site-spin basis $i \equiv (\mathbf{i}, \sigma_i)$ is given by:

$$\hat{H} = h \sum_{\sigma} \sum_{i \neq j} \hat{d}_{i\sigma}^{\dagger} \hat{d}_{j\sigma} + U \sum_i \hat{n}_{i\uparrow} \hat{n}_{i\downarrow} - \mu \sum_{i\sigma} \hat{n}_{i\sigma}, \quad (15)$$

where h is the hopping parameter (subsequently set to 1), U is the on-site repulsion and $\hat{n}_{i\sigma} = \hat{d}_{i\sigma}^{\dagger} \hat{d}_{i\sigma}$. The chemical potential is fixed at $\mu = \frac{U}{2}$. The density matrix at half-filling is specified by a single parameter a and reads in the site basis:

$$\rho_{\sigma}^{<} = \begin{pmatrix} \frac{1}{2} & a \\ a & \frac{1}{2} \end{pmatrix}. \quad (16)$$

The Hartree-Fock Hamiltonian is independent of a and is identical to the hopping part of the Hamiltonian:

$$h_{\text{HF}} = \begin{pmatrix} 0 & h \\ h & 0 \end{pmatrix}, \quad (17)$$

with eigenvalues $\epsilon_i^{\text{HF}} = \pm h$.

At equilibrium, the isolated system has been studied using a large number of approximations. Its spectral density (see Fig. 1 of Ref. [9], Fig. 6 of Ref. [21] or Fig. 13 of Ref. [8]) consists of two quasiparticle peaks with energies $\epsilon_i \xrightarrow{U \rightarrow 0} \epsilon_i^{\text{HF}}$, each accompanied by a satellite peak. In the atomic limit, i.e., as $h/U \rightarrow 0$, the spectral weight is equally distributed between the peaks. We probe the system by connecting it to two leads and applying the bias voltage $V_2(t)$ to the second lead. For negative or positive biases, occupied or unoccupied states are probed, respectively (Fig. 1, right).

Under equilibrium conditions the electronic density is stationary and, in general, deviates from the form (16) due to the tunneling to the leads in the presence of electronic correlations. The simplest, albeit numerically demanding, way to obtain the equilibrium density is by applying the adiabatic switching procedure, in which the electron interaction and the tunneling matrices become time-dependent, i.e., $U(t) = s_0(t)U$, $T_{ik\alpha}(t) = s_{\alpha}(t)T_{ik\alpha}$, typically we use the ramp functions of the form $s_{\alpha}(t) = \cos(\pi/2 \cdot t/t_i)^2 \theta(-t) + \theta(t)$, which build up correlations in the system over the time interval $[t_i, 0]$.

2.3 Time-dependent and steady-state currents

Since in GKBA formalism the collision integrals are known, time-dependent currents can be determined directly from the Meir-Wingreen formula [35, 36]

$$J_{\alpha}(t) = 2 \text{Re Tr}[I_{\alpha}(t)], \quad (18)$$

where $I^{\text{em}}(t) = \sum_{\alpha} I_{\alpha}(t)$, and individual contributions of each lead $I_{\alpha}(t)$ are determined from the $\mathcal{G}_{\ell\alpha}^{\text{em}}(t)$ correlator (14) in the case of GKBA, and from several correlators in the case of *i*GKBA [30].

Under stationary conditions, the steady-state currents in noninteracting systems or systems treated at the mean-field level can be determined from the Landauer-Büttiker (LB) formula [28]

$$J_{\alpha} = \int \frac{d\omega}{2\pi} \sum_{\beta} (f_{\alpha}(\omega - V_{\alpha}) - f_{\beta}(\omega - V_{\beta})) \times \text{Tr}[\Gamma_{\alpha}(\omega - V_{\alpha})G_0^{\text{R}}(\omega)\Gamma_{\beta}(\omega - V_{\beta})G_0^{\text{A}}(\omega)]. \quad (19)$$

Here, f_{α} and f_{β} are the distribution functions associated with leads α and β , respectively, and $G_0^{\text{A/R}}$ are the equilibrium mean-field advanced/retarded Green's functions of the central system. Extensions of this result to transient scenarios have also been demonstrated within the wide-band limit approximation [40, 41] with further generalizations [42–45].

Once the density matrix is known, mean-field currents can be easily computed using Eq. (19). This follows from the fact that, at the Hartree-Fock level, the electron self-energy consists only of the embedding part, $\Sigma(\omega) = \Sigma_{\text{em}}(\omega) = \sum_{\alpha} \Sigma_{\alpha}(\omega)$, where

$$\text{Im } \Sigma_{\alpha}^{\text{R}}(\omega) = -\frac{1}{2}\Gamma_{\alpha}(\omega), \quad \text{Re } \Sigma_{\alpha}^{\text{R}}(\omega) = \frac{1}{2}\mathcal{H}[\Gamma_{\alpha}](\omega). \quad (20)$$

Here, \mathcal{H} is the Hilbert transform:

$$\mathcal{H}[x](\omega) = \frac{1}{\pi} \mathcal{P} \int_{-\infty}^{\infty} d\nu \frac{x(\nu)}{\omega - \nu}. \quad (21)$$

We have then

$$G_0^{\text{R}}(\omega) = \frac{1}{\omega - h_{\text{HF}} - \Sigma^{\text{R}}(\omega)}, \quad (22)$$

and $G_0^{\text{A}}(\omega) = [G_0^{\text{R}}(\omega)]^{\dagger}$.

Despite being applicable only to noninteracting system, Eq. (19) represents a useful starting point for understanding more complicated interacting and time-dependent scenarios. On its basis it can be concluded that the current is non-zero if there is a non-zero overlap between $f_{\alpha} - f_{\beta}$, the spectral densities Γ_{α} , Γ_b and the density of states of the central system. By varying the energy position ϵ_{α} of a narrow-band left lead ($\alpha = 1$), and using a wide-band $\Omega_{\beta} \rightarrow \infty$ right lead ($\beta = 2$), the desired energy selectivity can be achieved.

It should be noted that Eq. (19) is not the only way to understand spectral properties. In a series of papers G. Cohen *et al.* [46, 47] gave a prescription how the spectral function of a system can be determined starting the Meir-Wingreen expression for the

steady-state current [28]:

$$J_\alpha = -2i \int \frac{d\omega}{2\pi} \text{Tr} [\Sigma_\alpha^<(\omega) A(\omega) - \Gamma_\alpha(\omega) G^<(\omega)], \quad (23)$$

where the lesser component of the lead specific embedding self-energy can be expressed in terms of the distribution function $f_\alpha(\omega)$ and the tunneling rate matrix $\Gamma_\alpha(\omega)$ as $\Sigma_\alpha^<(\omega) = if_\alpha(\omega)\Gamma_\alpha(\omega)$, but $G^<(\omega)$ is not known within GKBA. Unlike the Landauer–Büttiker formula, this approach does not require the assumption of a non-interacting system: the unknown lesser Green’s function is eliminated by taking the difference between currents computed using fully occupied and completely empty auxiliary leads at varying energy positions. This technique—varying the energy positions of two auxiliary leads—is complementary to the approach of varying a single lead’s chemical potential. The latter idea is more similar to the surface tunneling spectroscopy setup and in the context of GKBA was discussed in Ref. [48].

The method of G. Cohen *et al.* [46, 47], involving two auxiliary leads, provides a rigorous means of extracting the spectral function from measured currents. However, this scheme cannot be achieved in photoemission spectroscopies, as the occupation of detectors cannot be externally controlled. Therefore, in the present work, we consider a scenario involving multiple narrow-band leads at varying energy positions but fixed chemical potential (e.g., aligned with that of the central system). This setup enables exploration of the entire spectral range in a single simulation. We note that the two-lead auxiliary approach is fully compatible with the *i*GKBA formalism and will be employed in forthcoming systematic studies of electron correlation effects.

3 Results

We start with a weakly correlated case of $U = 1$, Fig. 2. The left lead is composed of 21 subleads of spectral widths $\Omega_{1,j} = 0.5$, centered at $\epsilon_{1,j} = -5 + 0.5(j - 1)$ for $1 \leq j \leq 21$. The right lead is centered at $\epsilon_2 = 0$, and its width is $\Omega_2 = 10$. The leads’ inverse temperatures for all calculations are fixed at $\beta_{1,j} = \beta_2 = 10$. The tunneling matrices in site basis are given by $\gamma_{1,j} = 0.05 \begin{pmatrix} 1 & 0 \\ 0 & 0 \end{pmatrix}$ and $\gamma_2 = 0.07 \begin{pmatrix} 0 & 0 \\ 0 & 1 \end{pmatrix}$. In panel (a), the composite spectral function (its trace) of the left lead $[\Gamma_1(\omega)]$ is compared with the spectral function of the right lead $[\Gamma_2(\omega)]$. The system is driven by the bias voltage $V_2(t)$ according to the following protocol:

$$V_2(t) = -2 + 4[1 + \exp(-25t)]^{-1}. \quad (24)$$

This means that during the adiabatic switching the system is subject to $V_2(t) = -2$. Then, at $t \sim 0$, the bias very quickly (on the order of 0.04 time units) changes its sign and the system evolves under $V_2(t) = 2$. In panel (b), the mean-field (HF, dashed lines) and the second Born approximation (2BA, solid lines) total ($\text{Tr}[\rho_\sigma^<]$) and natural (eigenvalues of the density matrix $\rho_\sigma^<$) occupations are compared. During the first time-interval the system loses approximately 0.4 electrons in each spin channel and during the second time-interval the system reaches 1.4 total number of electrons. Both

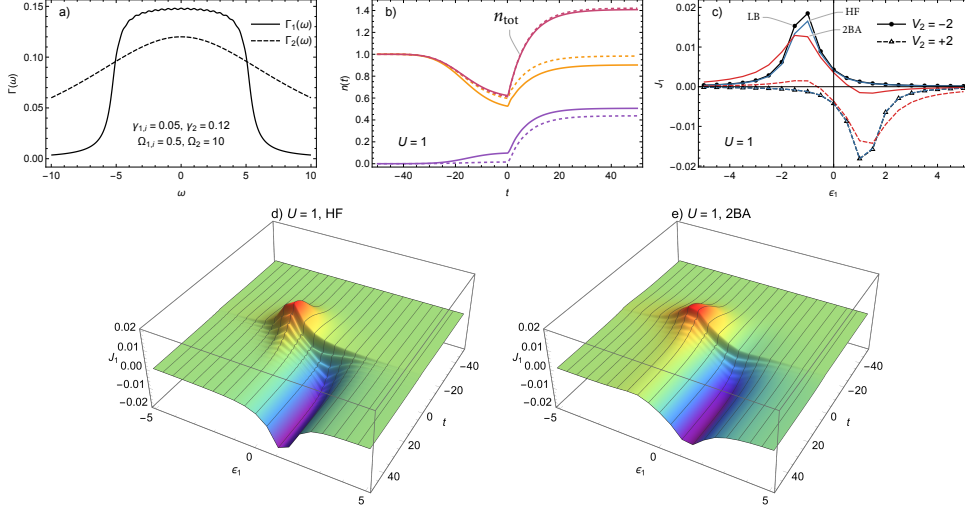


Fig. 2 Weakly correlated Hubbard dimer with $U = 1$. Top: a) spectral function of the leads, b) evolution of natural occupations (purple and orange), total number of electrons in the central system, dashed lines — Hartree-Fock, solid lines — second Born approximation, and c) energy-dependent currents through the left lead at stationary states corresponding to two bias voltages V_2 applied to the right lead; The currents are computed for predetermined energies $\epsilon_{1,j}$ of the subleads, continuous lines are a guide to the eye. Bottom: time- and energy-resolved currents through the left lead using d) the Hartree-Fock and e) second Born approximations.

approximations are consistent in the value of total occupation $n_{\text{tot}}(t)$, but they differ with respect to the natural occupations.

In Fig. 2(c), currents at $t = -1$ and $t = t_f$ (end of propagation) are compared. The LB currents are computed using the HF electron density matrix, they are in a good agreement with the HF currents obtained by the time propagation. Small deviations for $V_2 = -2$ are explained by incomplete thermalisation during the first time interval. For the second time-interval, the system thermalizes faster because it starts with already a correlated state from the first time-interval. 2BA results (red lines) closely agree with the HF results (blue lines), whereas peaks are slightly broader. Energy- and time-resolved currents are compared in panels (d) and (e), showing similarity between HF and 2BA in the weakly correlated case.

For calculations in the moderately- ($U = 5$) and strongly-correlated ($U = 10$) regimes, Figs. 3 and 4, slightly different lead parameters are selected: in order to increase the energy resolution we reduce the coupling $\gamma_2 = 0.07$ and the width of subleads $\Omega_{1,j} = 0.1$. However, to be able to cover the energy interval from -3 to 3 , the number of subleads is increased to 28, such that they are positioned at $\epsilon_{1,j} = -2.7 + 0.2(j - 1)$.

There are three pronounced effects of electronic correlations: i) A substantial broadening of the current peaks (panel c). ii) As a consequence, there is a suppression of the transient current oscillations (panel e), which are highly pronounced in the Hartree-Fock case (panel d). As explained in Ref. [28, 40, 41], these oscillations originate from virtual transitions between the resonant levels of the central system and

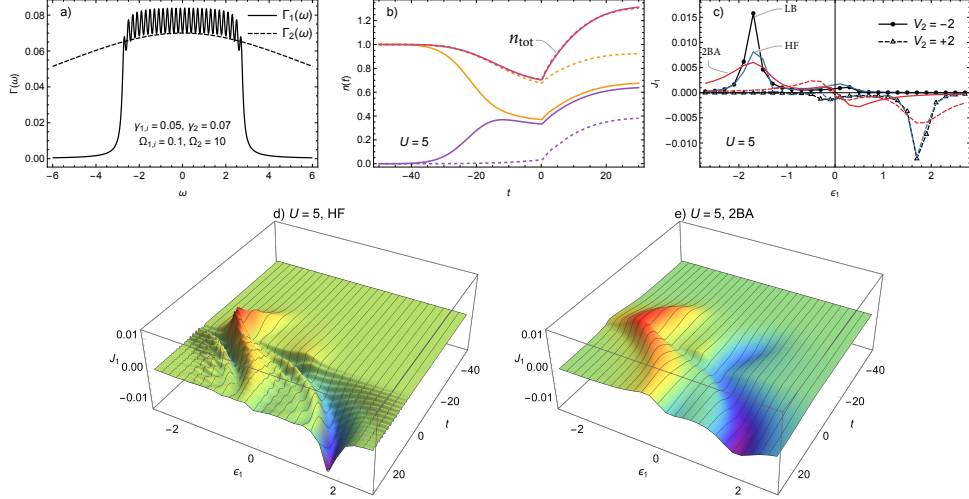


Fig. 3 Moderately correlated Hubbard dimer with $U = 5$. Top: a) spectral function of the leads, b) evolution of natural occupations (purple and orange), total number of electrons in the central system, dashed lines — Hartree-Fock, solid lines — second Born approximation, and c) energy-dependent currents through the left lead at stationary states corresponding to two bias voltages V_2 applied to the right lead; The currents are computed for predetermined energies $\epsilon_{1,j}$ of the subleads, continuous lines are a guide to the eye. Bottom: time- and energy-resolved currents through the left lead using d) the Hartree-Fock and e) second Born approximations.

the Fermi level of the biased reservoirs. Full Kadanoff-Baym calculations for isolated Hubbard clusters similarly demonstrate a suppression of the density oscillations at the fully self-consistent 2BA level (Fig. 4(d) of Ref. [49]). iii) Finally, the position of the peaks varies significantly during the time evolution. This aspect can be attributed to the large contribution of the mean-field potential at large U -values and a substantial evolution of the total electron density (panel b). Remarkably, the total electron occupation of the Hubbard dimer is not sensitive to the choice of method, as also observed in Ref. [50, 51].

The contribution of satellite peaks to the electron current is a separate and complicated issue. We were unable to resolve them at $U = 1$ because, in this case, the spectral weight of the satellites is small. For larger U -values, the satellites approach the main quasiparticle peak, requiring higher energy resolution. A good reference point would be the KBE calculations of Ref. [49, 52]. Comprehensive identification of all correlation features is a major undertaking and will be addressed in forthcoming publications.

4 Conclusions

In this work, we demonstrate the feasibility of accessing the time- and energy-resolved spectral density of a two-site Hubbard model using a nonequilibrium Green's function formalism. Our approach avoids the computationally demanding solution of the full two-time Kadanoff-Baym equation. Instead, we rely on a time-linear ODE approach for open-quantum systems based on the iterative GKBA reconstruction (*i*GKBA) [30]. The spectral density is accessed by bringing the system into contact with two leads and

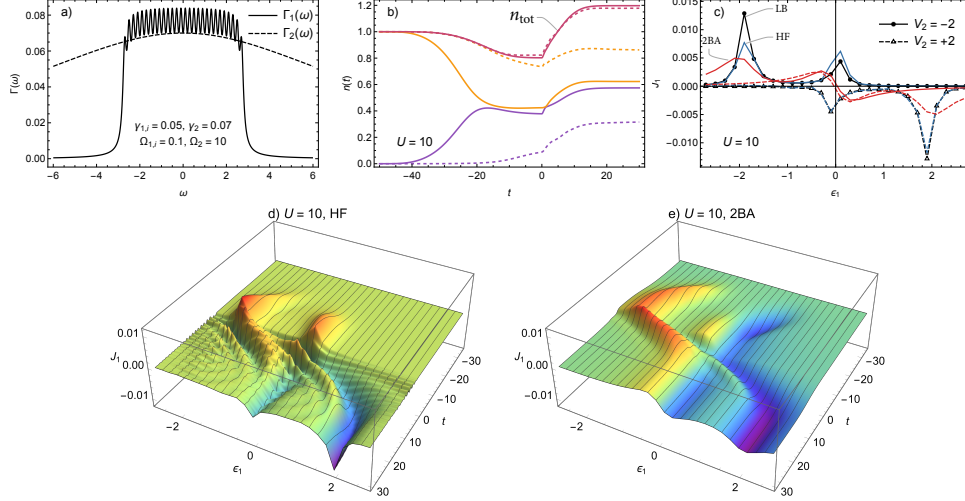


Fig. 4 Strongly correlated Hubbard dimer with $U = 10$. Top: a) spectral function of the leads, b) evolution of natural occupations (purple and orange), total number of electrons in the central system, dashed lines — Hartree-Fock, solid lines — second Born approximation, and c) energy-dependent currents through the left lead at stationary states corresponding to two bias voltages V_2 applied to the right lead; The currents are computed for predetermined energies $\epsilon_{1,j}$ of the subleads, continuous lines are a guide to the eye. Bottom: time- and energy-resolved currents through the left lead using d) the Hartree-Fock and e) second Born approximations.

computing the electron current through the narrow-band leads. This setup directly mimics a photoemission experiment. Under stationary conditions, the results of the simulations are interpreted using the Landauer-Büttiker formula. We demonstrate electronic correlations-induced shifts of energy levels and their broadening, as well as the suppression of oscillations in transient currents — effects known to affect equilibrium transport [53] or observed in time-dependent quantum transport through the use of computationally extensive embedded Kadanoff-Baym method [54].

Acknowledgements. R.T. acknowledges the financial support of the Research Council of Finland through the Finnish Quantum Flagship (Project No. 359240) and the Jane and Aatos Erkko Foundation (Project EffQSim).

Data availability

Manuscript has no associated data.

References

- [1] Hubbard, J.: Electron Correlations in Narrow Energy Bands. Proc. R. Soc. London, Ser. A **276**(1365), 238–257 (1963)

- [2] Esslinger, T.: Fermi-Hubbard Physics with Atoms in an Optical Lattice. *Annu. Rev. Condens. Matter Phys.* **1**(1), 129–152 (2010) <https://doi.org/10.1146/annurev-conmatphys-070909-104059>
- [3] Bertini, B., Heidrich-Meisner, F., Karrasch, C., Prosen, T., Steinigeweg, R., Žnidarič, M.: Finite-temperature transport in one-dimensional quantum lattice models. *Rev. Mod. Phys.* **93**(2), 025003 (2021) <https://doi.org/10.1103/RevModPhys.93.025003>
- [4] Brantut, J.-P., Grenier, C., Meineke, J., Stadler, D., Krinner, S., Kollath, C., Esslinger, T., Georges, A.: A Thermoelectric Heat Engine with Ultracold Atoms. *Science* **342**(6159), 713–715 (2013) <https://doi.org/10.1126/science.1242308>
- [5] Karrasch, C., Kennes, D.M., Heidrich-Meisner, F.: Thermal Conductivity of the One-Dimensional Fermi-Hubbard Model. *Phys. Rev. Lett.* **117**(11), 116401 (2016) <https://doi.org/10.1103/PhysRevLett.117.116401>
- [6] Pavlyukh, Y.: Nonequilibrium Dynamics of the Hubbard Dimer. *Phys. Status Solidi B*, 2300510 (2024) <https://doi.org/10.1002/pssb.202300510>
- [7] Romaniello, P., Guyot, S., Reining, L.: The self-energy beyond GW: Local and nonlocal vertex corrections. *J. Chem. Phys.* **131**(15), 154111 (2009) <https://doi.org/10.1063/1.3249965>
- [8] Carrascal, D.J., Ferrer, J., Smith, J.C., Burke, K.: The Hubbard dimer: a density functional case study of a many-body problem. *J. Phys. Condens. Matter* **27**(39), 393001 (2015) <https://doi.org/10.1088/0953-8984/27/39/393001>
- [9] Di Sabatino, S., Loos, P.-F., Romaniello, P.: Scrutinizing GW-Based Methods Using the Hubbard Dimer. *Frontiers in Chemistry* **9**, 751054 (2021) <https://doi.org/10.3389/fchem.2021.751054>
- [10] Lipavský, P., Špička, V., Velický, B.: Generalized Kadanoff-Baym ansatz for deriving quantum transport equations. *Phys. Rev. B* **34**(10), 6933–6942 (1986) <https://doi.org/10.1103/PhysRevB.34.6933>
- [11] Schlünzen, N., Joost, J.-P., Bonitz, M.: Achieving the Scaling Limit for Nonequilibrium Green Functions Simulations. *Phys. Rev. Lett.* **124**(7), 076601 (2020) <https://doi.org/10.1103/PhysRevLett.124.076601>
- [12] Joost, J.-P., Schlünzen, N., Bonitz, M.: G1-G2 scheme: Dramatic acceleration of nonequilibrium Green functions simulations within the Hartree-Fock generalized Kadanoff-Baym ansatz. *Phys. Rev. B* **101**(24), 245101 (2020) <https://doi.org/10.1103/PhysRevB.101.245101>
- [13] Pavlyukh, Y., Perfetto, E., Stefanucci, G.: Photoinduced dynamics of organic

- molecules using nonequilibrium Green's functions with second-Born, GW , T -matrix, and three-particle correlations. Phys. Rev. B **104**(3), 035124 (2021) <https://doi.org/10.1103/PhysRevB.104.035124>
- [14] Cundiff, S.T., Mukamel, S.: Optical multidimensional coherent spectroscopy. Phys. Today **66**(7), 44–49 (2013) <https://doi.org/10.1063/PT.3.2047>
 - [15] Cheng, Y.-C., Fleming, G.R.: Dynamics of Light Harvesting in Photosynthesis. Annu. Rev. Phys. Chem. **60**(1), 241–262 (2009) <https://doi.org/10.1146/annurev.physchem.040808.090259>
 - [16] Huang, D., Sampson, K., Ni, Y., Liu, Z., Liang, D., Watanabe, K., Taniguchi, T., Li, H., Martin, E., Levinsen, J., Parish, M.M., Tutuc, E., Efimkin, D.K., Li, X.: Quantum Dynamics of Attractive and Repulsive Polarons in a Doped MoSe 2 Monolayer. Phys. Rev. X **13**(1), 011029 (2023) <https://doi.org/10.1103/PhysRevX.13.011029>
 - [17] Schuurman, M.S., Blanchet, V.: Time-resolved photoelectron spectroscopy: the continuing evolution of a mature technique. Phys. Chem. Chem. Phys. **24**(34), 20012–20024 (2022) <https://doi.org/10.1039/D1CP05885A>
 - [18] Huang, C., Duan, S., Zhang, W.: High-resolution time- and angle-resolved photoemission studies on quantum materials. Quantum Frontiers **1**(1), 15 (2022) <https://doi.org/10.1007/s44214-022-00013-x>
 - [19] Schüler, M., Berakdar, J., Pavlyukh, Y.: Time-dependent many-body treatment of electron-boson dynamics: Application to plasmon-accompanied photoemission. Phys. Rev. B **93**(5), 054303 (2016) <https://doi.org/10.1103/PhysRevB.93.054303>
 - [20] Pavlyukh, Y., Perfetto, E., Karlsson, D., Leeuwen, R., Stefanucci, G.: Time-linear scaling nonequilibrium Green's function methods for real-time simulations of interacting electrons and bosons. I. Formalism. Phys. Rev. B **105**(12), 125134 (2022) <https://doi.org/10.1103/PhysRevB.105.125134>
 - [21] Romaniello, P., Bechstedt, F., Reining, L.: Beyond the GW approximation: Combining correlation channels. Phys. Rev. B **85**(15), 155131 (2012) <https://doi.org/10.1103/PhysRevB.85.155131>
 - [22] Schlünzen, N., Joost, J.-P., Heidrich-Meisner, F., Bonitz, M.: Nonequilibrium dynamics in the one-dimensional Fermi-Hubbard model: Comparison of the nonequilibrium Green-functions approach and the density matrix renormalization group method. Phys. Rev. B **95**(16), 165139 (2017) <https://doi.org/10.1103/PhysRevB.95.165139>
 - [23] Schlünzen, N., Hermanns, S., Scharnke, M., Bonitz, M.: Ultrafast dynamics of strongly correlated fermions—nonequilibrium Green functions and self-energy approximations. J. Phys. Condens. Matter **32**(10), 103001 (2020) <https://doi.org/10.1088/1361-6480/ab5555>

[//doi.org/10.1088/1361-648X/ab2d32](https://doi.org/10.1088/1361-648X/ab2d32)

- [24] Karlsson, D., Leeuwen, R., Pavlyukh, Y., Perfetto, E., Stefanucci, G.: Fast Green's Function Method for Ultrafast Electron-Boson Dynamics. *Phys. Rev. Lett.* **127**(3), 036402 (2021) <https://doi.org/10.1103/PhysRevLett.127.036402>
- [25] Tuovinen, R., Pavlyukh, Y., Perfetto, E., Stefanucci, G.: Time-Linear Quantum Transport Simulations with Correlated Nonequilibrium Green's Functions. *Phys. Rev. Lett.* **130**(24), 246301 (2023) <https://doi.org/10.1103/PhysRevLett.130.246301>
- [26] Pavlyukh, Y., Perfetto, E., Stefanucci, G.: Interacting electrons and bosons in the doubly screened \widetilde{GW} approximation: A time-linear scaling method for first-principles simulations. *Phys. Rev. B* **106**(20), 201408 (2022) <https://doi.org/10.1103/PhysRevB.106.L201408>
- [27] Tuovinen, R., Pavlyukh, Y.: Electroluminescence Rectification and High Harmonic Generation in Molecular Junctions. *Nano Lett.* **24**(29), 9096–9103 (2024) <https://doi.org/10.1021/acs.nanolett.4c02609>
- [28] Stefanucci, G., Leeuwen, R.: Nonequilibrium Many-Body Theory of Quantum Systems: A Modern Introduction. Cambridge University Press, Cambridge (2013)
- [29] Hu, J., Xu, R.-X., Yan, Y.: Communication: Padé spectrum decomposition of Fermi function and Bose function. *J. Chem. Phys.* **133**, 101106 (2010) <https://doi.org/10.1063/1.3484491>
- [30] Pavlyukh, Y., Tuovinen, R.: Open system dynamics in linear time beyond the wide-band limit. *Phys. Rev. B* **111**(24), 241101 (2025) <https://doi.org/10.1103/PhysRevB.111.L241101>
- [31] Kalvová, A., Velický, B., Špička, V.: Beyond the Generalized Kadanoff-Baym Ansatz. *Phys. Status Solidi B* **256**(7), 1800594 (2019) <https://doi.org/10.1002/pssb.201800594>
- [32] Kalvová, A., Špička, V., Velický, B., Lipavský, P.: Dynamical vertex correction to the generalized Kadanoff-Baym Ansatz. *Europhys. Lett.* **141**(1), 16002 (2023) <https://doi.org/10.1209/0295-5075/acad9b>
- [33] Kalvová, A., Špička, V., Velický, B., Lipavský, P.: Fast corrections to the generalized Kadanoff-Baym ansatz. *Phys. Rev. B* **109**(13), 134306 (2024) <https://doi.org/10.1103/PhysRevB.109.134306>
- [34] Kalvová, A., Lipavský, P.: Short-time character of corrections to the generalized Kadanoff-Baym Ansatz. *Eur. Phys. J. B* **98**(5), 86 (2025) <https://doi.org/10.1140/epjb/s10051-025-00938-x>

- [35] Meir, Y., Wingreen, N.S.: Landauer formula for the current through an interacting electron region. *Phys. Rev. Lett.* **68**(16), 2512–2515 (1992) <https://doi.org/10.1103/PhysRevLett.68.2512>
- [36] Jauho, A.-P., Wingreen, N.S., Meir, Y.: Time-dependent transport in interacting and noninteracting resonant-tunneling systems. *Phys. Rev. B* **50**(8), 5528–5544 (1994) <https://doi.org/10.1103/PhysRevB.50.5528>
- [37] Schüler, M., Pavlyukh, Y.: Spectral properties from Matsubara Green’s function approach: Application to molecules. *Phys. Rev. B* **97**(11), 115164 (2018) <https://doi.org/10.1103/PhysRevB.97.115164>
- [38] Dong, X., Zgid, D., Gull, E., Strand, H.U.R.: Legendre-spectral Dyson equation solver with super-exponential convergence. *J. Chem. Phys.* **152**(13), 134107 (2020) <https://doi.org/10.1063/5.0003145>
- [39] Fei, J., Yeh, C.-N., Gull, E.: Nevanlinna Analytical Continuation. *Phys. Rev. Lett.* **126**(5), 056402 (2021) <https://doi.org/10.1103/PhysRevLett.126.056402>
- [40] Tuovinen, R., Leeuwen, R., Perfetto, E., Stefanucci, G.: Time-dependent Landauer-Büttiker formula for transient dynamics. *J. Phys. Conf. Ser.* **427**, 012014 (2013) <https://doi.org/10.1088/1742-6596/427/1/012014>
- [41] Tuovinen, R., Perfetto, E., Stefanucci, G., Van Leeuwen, R.: Time-dependent Landauer-Büttiker formula: Application to transient dynamics in graphene nanoribbons. *Phys. Rev. B* **89**(8), 085131 (2014) <https://doi.org/10.1103/PhysRevB.89.085131>
- [42] Ridley, M., MacKinnon, A., Kantorovich, L.: Current through a multilead nano-junction in response to an arbitrary time-dependent bias. *Phys. Rev. B* **91**(12), 125433 (2015) <https://doi.org/10.1103/PhysRevB.91.125433>
- [43] Ridley, M., MacKinnon, A., Kantorovich, L.: Fluctuating-bias controlled electron transport in molecular junctions. *Phys. Rev. B* **93**(20), 205408 (2016) <https://doi.org/10.1103/PhysRevB.93.205408>
- [44] Ridley, M., Talarico, N.W., Karlsson, D., Lo Gullo, N., Tuovinen, R.: A many-body approach to transport in quantum systems: from the transient regime to the stationary state. *J. Phys. A* **55**(27), 273001 (2022) <https://doi.org/10.1088/1751-8121/ac7119>
- [45] Ridley, M., Bellasai, L., Moskalets, M., Kantorovich, L., Tuovinen, R.: Photon-assisted stochastic resonance in nanojunctions. *Phys. Rev. B* **111**(9), 094309 (2025) <https://doi.org/10.1103/PhysRevB.111.094309>
- [46] Cohen, G., Gull, E., Reichman, D.R., Millis, A.J.: Green’s Functions from Real-Time Bold-Line Monte Carlo Calculations: Spectral Properties of the

- Nonequilibrium Anderson Impurity Model. *Phys. Rev. Lett.* **112**(14), 146802 (2014) <https://doi.org/10.1103/PhysRevLett.112.146802>
- [47] Cohen, G., Reichman, D.R., Millis, A.J., Gull, E.: Green's functions from real-time bold-line Monte Carlo. *Phys. Rev. B* **89**(11), 115139 (2014) <https://doi.org/10.1103/PhysRevB.89.115139>
 - [48] Cosco, F., Tuovinen, R., Lo Gullo, N.: Interacting Electrons in a Flat-Band System within the Generalized Kadanoff-Baym Ansatz. *Phys. Status Solidi B* **261**(9), 2300561 (2024) <https://doi.org/10.1002/pssb.202300561>
 - [49] Friesen, M.P., Verdozzi, C., Almbladh, C.-O.: Successes and Failures of Kadanoff-Baym Dynamics in Hubbard Nanoclusters. *Phys. Rev. Lett.* **103**(17), 176404 (2009) <https://doi.org/10.1103/PhysRevLett.103.176404>
 - [50] Uimonen, A.-M., Khosravi, E., Stan, A., Stefanucci, G., Kurth, S., Leeuwen, R., Gross, E.K.U.: Comparative study of many-body perturbation theory and time-dependent density functional theory in the out-of-equilibrium Anderson model. *Phys. Rev. B* **84**(11), 115103 (2011) <https://doi.org/10.1103/PhysRevB.84.115103>
 - [51] Khosravi, E., Uimonen, A.-M., Stan, A., Stefanucci, G., Kurth, S., Van Leeuwen, R., Gross, E.K.U.: Correlation effects in bistability at the nanoscale: Steady state and beyond. *Phys. Rev. B* **85**(7), 075103 (2012) <https://doi.org/10.1103/PhysRevB.85.075103>
 - [52] Puig Von Friesen, M., Verdozzi, C., Almbladh, C.-O.: Kadanoff-Baym dynamics of Hubbard clusters: Performance of many-body schemes, correlation-induced damping and multiple steady and quasi-steady states. *Phys. Rev. B* **82**(15), 155108 (2010) <https://doi.org/10.1103/PhysRevB.82.155108>
 - [53] Strange, M., Rostgaard, C., Häkkinen, H., Thygesen, K.S.: Self-consistent GW calculations of electronic transport in thiol- and amine-linked molecular junctions. *Phys. Rev. B* **83**(11), 115108 (2011) <https://doi.org/10.1103/PhysRevB.83.115108>
 - [54] Myöhänen, P., Tuovinen, R., Korhonen, T., Stefanucci, G., Leeuwen, R.: Image charge dynamics in time-dependent quantum transport. *Phys. Rev. B* **85**(7), 075105 (2012) <https://doi.org/10.1103/PhysRevB.85.075105>